Observed Field Behaviour of Soft Clay Due to Embankment Loading: A Case Study in Queensland, Australia

E. Y. N. Oh
Queensland Dept. of Main Roads, Herston, Queensland, Australia
erwin.y.oh@mainroads.qld.gov.au

C. Surarak[1], A. S. Balasubramaniam[2] & M. Huang[3]
Griffith School of Engineering, Griffith University, Gold Coast, Queensland, Australia.
[1]*chanaton.surarak@student.griffith.edu.au,* [2]*a.bala@griffith.edu.au,* [3]*m.huang@griffith.edu.au*

Abstract: In this paper, the field behaviours of a trial embankment in Southeast Queensland are presented. The trial embankment is approximately 90m in length and 36m in width. It has two sections with vertical drains installed at a spacing of 1 m (Section A) and 2 m (Section C) triangular pattern, and a third section (Section B) without drains (control section). This trial embankment was constructed to observe the ground response upon loading, and evaluate the effectiveness of ground improvement techniques using vertical drains on the soft clays in this region. This paper presents the findings obtained from the field observations during construction. Deformation behaviour and pore pressure response below the instrumented embankment are investigated and the performance of vertical drains is discussed. This paper gives a classic case study of a trial embankment built on soft clay in Southeast Queensland, Australia.

1 INTRODUCTION

This paper presents the laboratory results and field behaviour of alluvial soft clay found in Sunshine Coast, Southeast Queensland. Soft clays are wide spread along the coastlines of Australia. They pose difficult problems in the design and construction of roads, expressways and motorways. By definition, soft clays are of low shear strength and high compressibility. Generally, they are sensitive and their strength is readily reduced by disturbance during sampling and testing.

The test embankment presented in this paper was fully instrumented to measure the settlements, lateral movements and the development of excess pore pressures and their dissipation with time under the embankment load. Also, ground improvement technique using prefabricated vertical drains (PVD) was also evaluated for their potential applications

2 SITE DESCRIPTION AND SOIL CONDITIONS

The trial embankment area had the deepest soft clay layers extending to approximately 11m depth. In this area, 33 boreholes were drilled up to 30m depth. Besides the boreholes, standard penetration tests (SPT), cone penetration tests (CPT), and field shear vane tests were conducted.

The soil strata can be classified into several layers. Field testing has indicated a substantial deposit of very soft compressible organic silty clay between 4m and 10m thick. This material is underlain by a layer of very loose silty sand of approximately 2 m thick. This in turn is underlain by moderately dense to dense sand (coffee rock) strata of 4 m to 6 m thick.

Fig.1 indicates typical sub-soil layers in the trial embankment area. In this figure, silty clay (CH) is found up to about 8m depth followed by clayey silt (MH), silty clay (CH) and clayey sand up to 12m depth. The natural water content of these layers were substantially higher than the liquid limit and the highest water content of 120% is found at 2m - 6.5m depth, followed by lower water content of about 80% from 6.5 m to 12 m depth. As such the weakest soft clay is encountered at 2 m - 6.5 m depth and this layer is bound to be of low shear strength as revealed from the natural water content. The liquidity index of the clay is higher than 1.0 as the natural water content is higher than the liquid limit. The plasticity index of the clay is uniform with depth and it is about 40%.

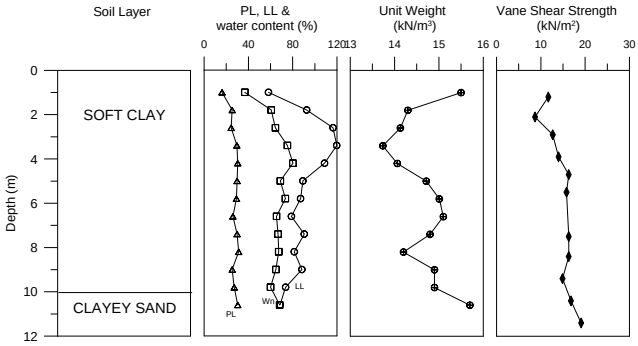

Fig. 1 Index properties, unit weight and vane shear strength

The voids ratio-effective vertical stress relationships for these tests are presented in Figs. 2(a), 2(b) and 2(c). From these voids ratio-effective stress relations, values of the compression index C_c, the coefficient of compressibility a_v, the coefficient of volume decrease m_v, the constraint modulus D and the coefficient of consolidation, C_v were established as a function of the effective vertical stress. The compression indexes for all samples (see Fig. 3) were found to increase with effective vertical stress initially and thereafter, it remains constant. Depending on the initial water content of the samples, the C_c vales generally ranged from 0.5 to 1.0 at stresses in the normally consolidated range. The exception was the sample taken at depth of 8.2 m to 9.0m, which indicated a C_c value of 1.5 in the normally consolidated range of stress levels.

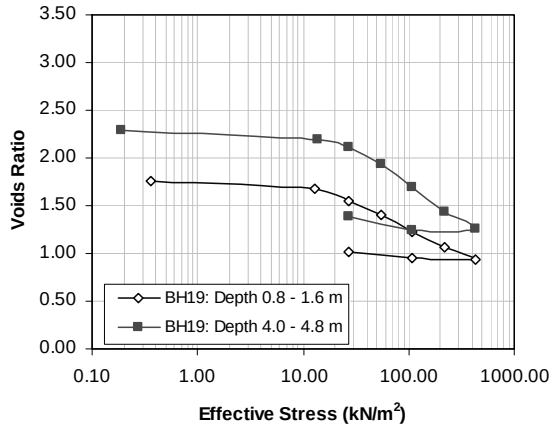

Fig. 2(a) Voids ratio – effective vertical stress for BH19

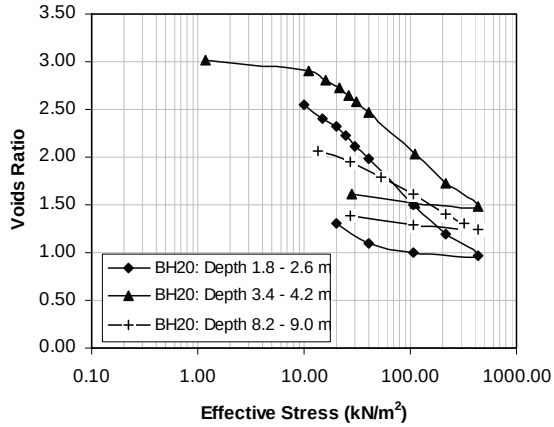

Fig. 2(b) Voids ratio – effective vertical stress for BH20

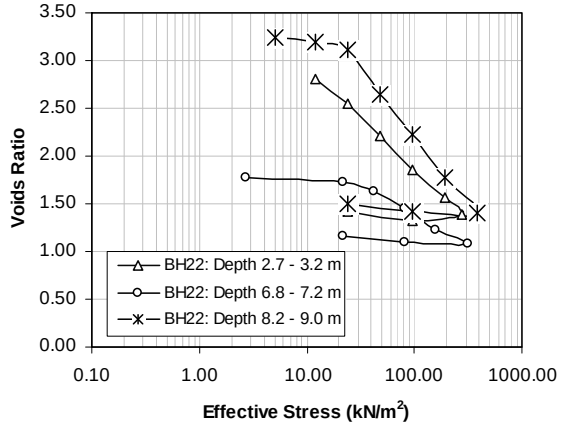

Fig. 2(c) Voids ratio – effective vertical stress for BH22

Fig. 4 illustrates the variation of the coefficient of volume decrease m_v, with increase in effective vertical stress. The m_v values at the lower stress range seem to have a large variation from 1 to 5 MN/m^2, but as the effective stress increases from 50 to 100 kN/m^2, the m_v values ranged from 1 to 3 MN/m^2 for most samples. In this figure, the m_v value of 2.2 MN/m^2 obtained from back-calculation based on the centreline settlement of Section A of the test embankment is also shown. This will be discussed at a latter section under the interpretations of settlements below the test embankment.

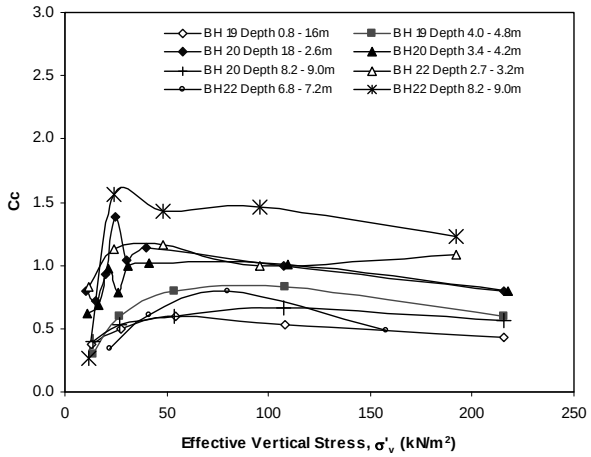

Fig. 3 Variation of compression index, C_C, with effective vertical stress, σ'_v

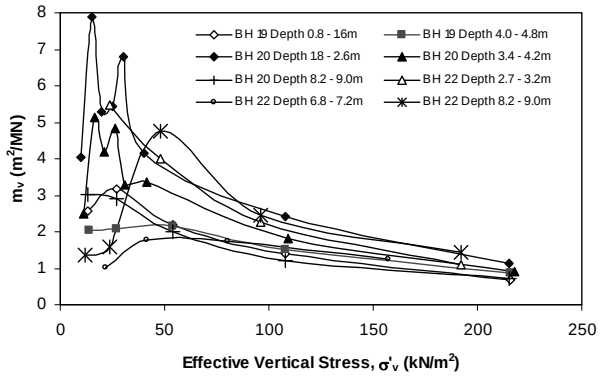

Fig. 4 Variation of coefficient of volume decrease, m_v, with effective vertical stress, σ'_v

3 TEST EMBANKMENT

The test embankment is approximately 90m in length and 36m in width. Vertical drains were installed with a crawler-mounted machine from the working platform. Section A and C of the test embankment are the prime sections representing the design vertical drain spacing (1m of triangular pattern) and no drains respectively. Section C representing an intermediate case with 2m triangular pattern drain spacing and less instruments.

3.1 *Instrumentation in Test Embankment*

The details of the cross sections and the instrumentations used are shown in Figs. 5, 6 and 7. It is noted that sensitive soft silty clay extends to about 10m depth followed by a 6 m thick layer of sand and below this is a 2m thick layer of sensitive clay which again is followed by sand.

3.2 *Interpretation of Settlement Data*

Horizontal profile gauges were installed in Section A and Section B to monitor the settlements across the sections with varying time period ranging from one day to 724 days. These hydraulic profile gauge data are presented in Fig. 8 for Section A and Section B, and they were interpreted extensively.

In the interpretation of these hydraulic profile gauges, there are 2 observations. Firstly, Section A with PVD, showed higher settlement at any time when compared with Section B without PVD. This is illustrated in Fig. 8 for time period of approximately, 1 day, 62 days, 93 days and 533 days. At all times, Sec-

tion A experienced higher settlement than Section B. Also individual settlement–log time plots are plotted for all sections show that Section A experienced greater settlement than Section B.

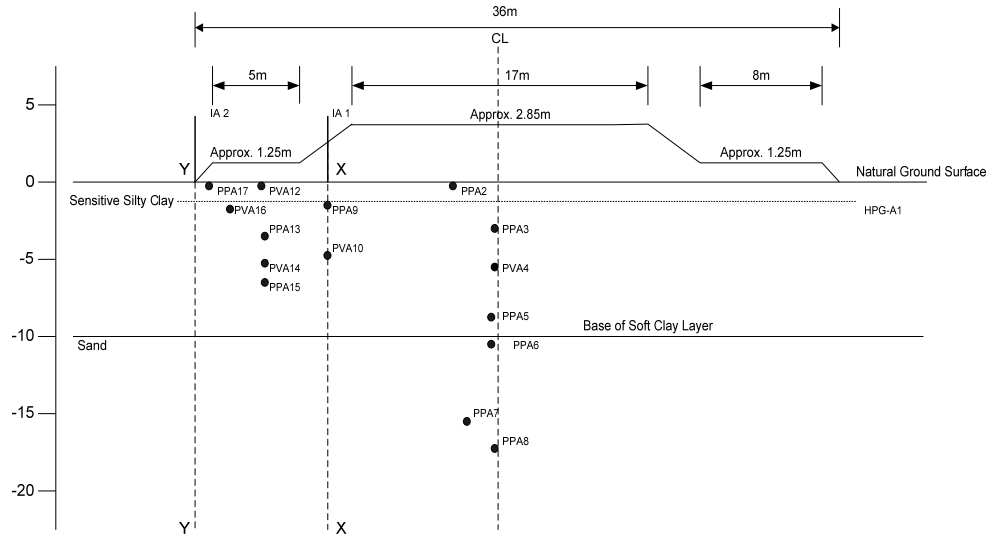

Fig. 5 Cross section showing instrumentation layout plan for Section A (PVD at 1m spacing)

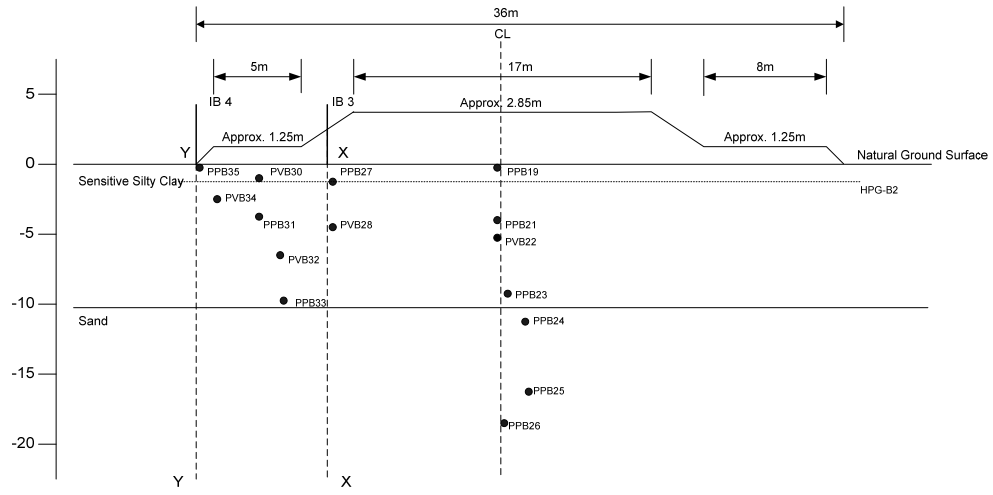

Fig. 6 Cross section showing instrumentation layout plan for Section B (control embankment)

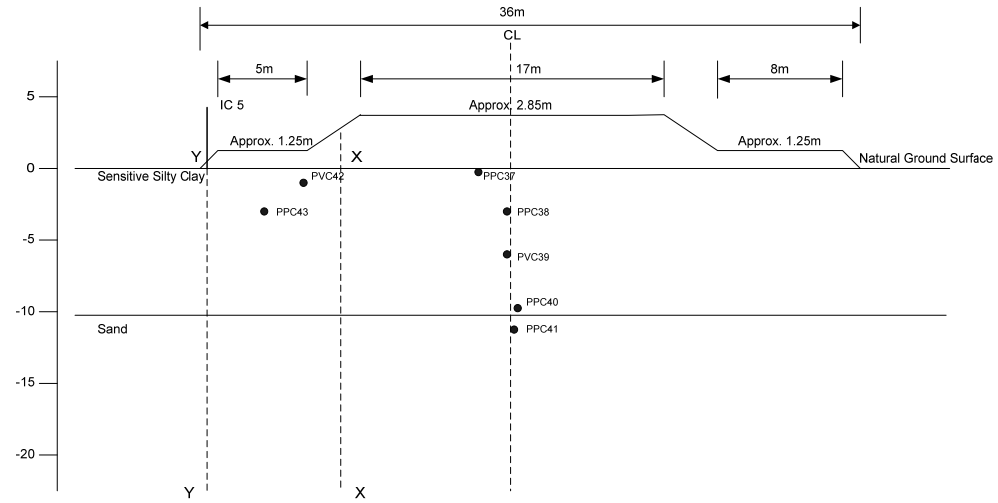

Fig. 7 Cross section showing instrumentation layout plan for Section C (PVD at 2m spacing)

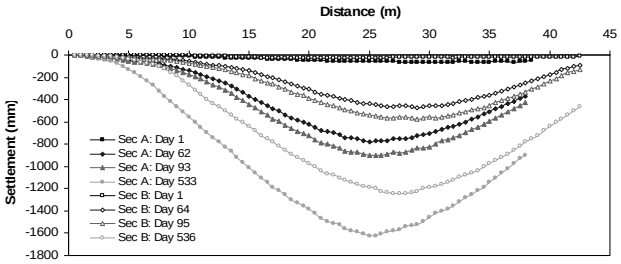

Fig. 8 Surface settlements from horizontal profile gauge in Section A and Section B

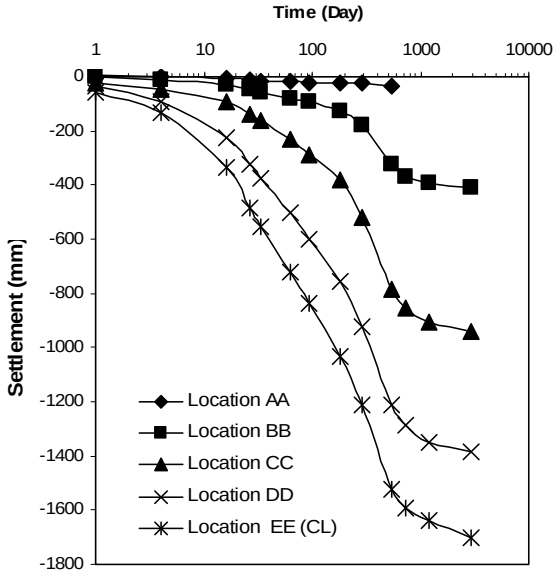

Fig. 9 Variation of settlement with time along the centerline and the locations to the left in Section A (100% Consolidation Completed)

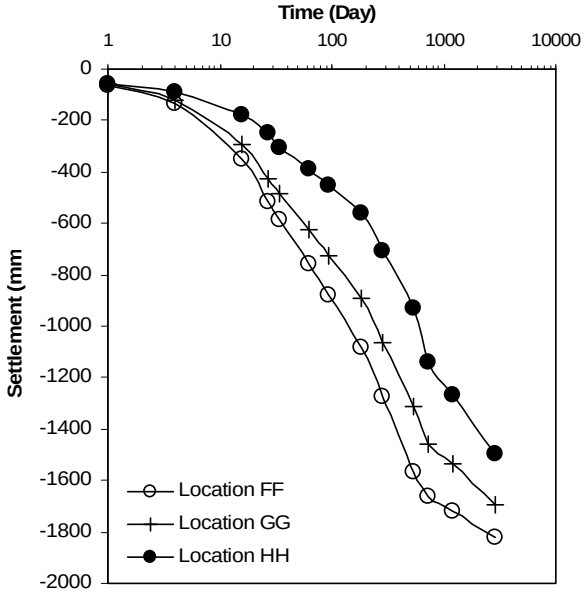

Fig. 10 Variation of settlement with time at the locations to the right of centerline in Section A (100% Consolidation Not Completed)

Secondly, Section A with the PVD, the settlement-log time plots indicated that 100% primary consolidation is over virtually for all sections, to the left of the centre line. But these plots indicate that the section to the right of the centre line were unable to achieve 100% primary consolidation even with the use of PVD in closer spacing of 1.0m. This observation is rather difficult to comprehend.

The above observation was established systematically, by plotting the settlement-log time plot of each location separately to the left and to the right of the centre line of Section A. The settlements for the centre line and the locations to the left are shown in Fig. 9; those corresponding to the right are shown in Fig. 10. The location marked EE corresponds to the centreline of the embankment. The locations DD, CC, BB and AA were taken from the centre line to the left at distances of 5m, 10m, 15m and 20m respectively. Similarly the locations FF, GG and HH were on the right hand side and at distances of 5m, 10m and 15m respectively away from the centreline.

The settlement-log time plot of each separate location to the left and to the right of the centre line of Section B is given in Fig. 11.

When the settlement-log time plot do not show an *S* curve, and where the Casagrande method cannot be applied to estimate the 100% primary consolidation, the Aasoka (1978) method was used to estimate the 100% primary consolidation. It was observed later that the Asaoka Method at times give lower values for the ultimate settlement.

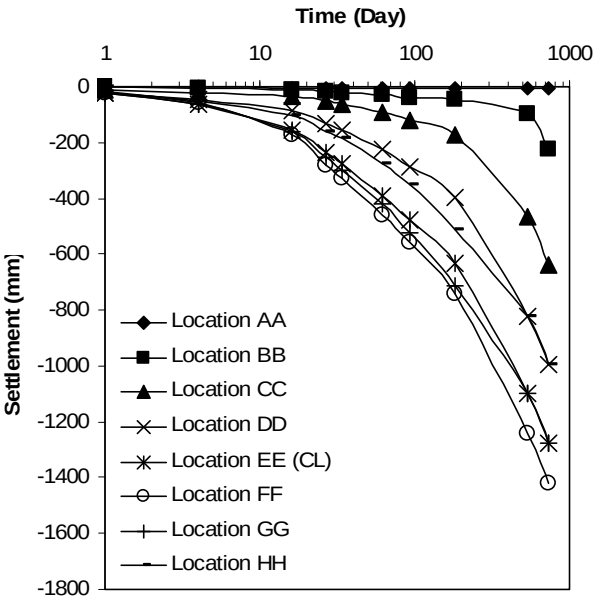

Fig. 11 Variation of settlement with time in Section B

Tables 1 and 2 summarise the 100% settlement estimated from the Casagrande and Asaoka methods for Section A and Section B respectively. These values indicate that even Section B is having proportionately higher settlements, even though no PVD were used. The major reason for this was perhaps due to the fact that the PVD Section A and Section C are on either side of the section B which have no PVD. Earlier work carried out at other sites in Southeast Asia and elsewhere indicated a better arrangement would have been to separately locate the PVD Sections and the no-PVD Section so that there is no interference effect. By not doing so at the test embankment presented here, the lateral drainage from the Section with no PVD (Section B) and through silt and sand lenses to the PVD in the drained sections have possibly occurred.

3.3 *Lateral Deformation from Inclinometer*

Lateral deformation profiles were determined at locations XX and YY (see Figs. 5, 6 and 7). However, only in Section A and Section B inclinometer casings were installed at the location XX. While for Section C, as well as for Section A and B, inclinometer casings were installed in YY. Fig. 12 illustrates the lateral deformation profiles for Section A and Section B at location XX after one day, 62 days, 93 days and 526 days. Initially, Section A with PVD was found to develop more lateral deformation. Perhaps this may be due to the disturbance created by the installation of PVD. However at 526 days time both Section A and Section B have similar lateral deformation profiles at XX.

Table 1 Ultimate settlement (100 percent consolidation settlement) in Section A

Location	Casagrande's Method 100 % Settlement (mm)	Asaoka's Method 100 % Settlement (mm)
CL	1570	-
5m Left from CL	1320	-
10m Left from CL	885	-
15m Left from CL	380	-
20m Left from CL	-	-
5m Right from CL	-	1506
10m Right from CL	-	1316
15m Right from CL	-	970

Table 2 Ultimate settlement (100 percent consolidation settlement) in Section B

Location	Casagrande's Method 100 pc Settlement (mm)	Asaoka's Method 100 pc Settlement (mm)
CL	-	1200
5m Left from CL	-	1050
10m Left from CL	-	480
15m Left from CL	-	290
20m Left from CL	-	-
5m Right from CL	-	1200
10m Right from CL	-	1060
15m Right from CL	-	830

3.4 *Excess Pore Pressure Development and Dissipation*

The locations of the piezometers in Section A, Section B and Section C were shown in Figs. 5, 6, and 7. It should be noted that the designation PV is used for the vibrating wire piezometers and the symbol PVA means the vibrating wire piezometer PV in Section A. Similarly, the symbol PP means pneumatic piezometer, and thus PPA refers to the pneumatic piezometer in Section A. Thus the last symbol of each piezometer designation indicates the relevant section in which the piezometer is located.

The excess pore pressures were determined along three alignments in Section A. The construction sequence adopted is shown in Fig. 13. The excess pore pressures as indicated by piezometers PVA4, PVA10 and PVA 14 are shown in Fig. 14. These piezometers are located around 5.5m depth and PVA4 is along the centre line of the Section, while PVA10 is along the location XX and PVA 14 is between locations XX and YY. It is noted that the piezometer PVA4 along the centre line indicates maximum excess pore pressures and this is followed by piezometer PVA 10 and the least excess pore pressure was indicated by piezometer PVA 14. These measurements are in accordance with the excess stress at these points due to the embankment loading.

For Section B, excess pore pressures are plotted in Fig. 15 along the centre line as indicated by piezometers PPB21 and PPB23 located at 4.5m and 9.5m depth respectively. Both piezometers indicate similar development of excess pore pressures and also dissipation pattern. Unlike the piezometers in Section A with PVD, the piezometers PPB21 and PPB 23 in Section B with no PVD did not indicate faster dissipation of excess pore pressures.

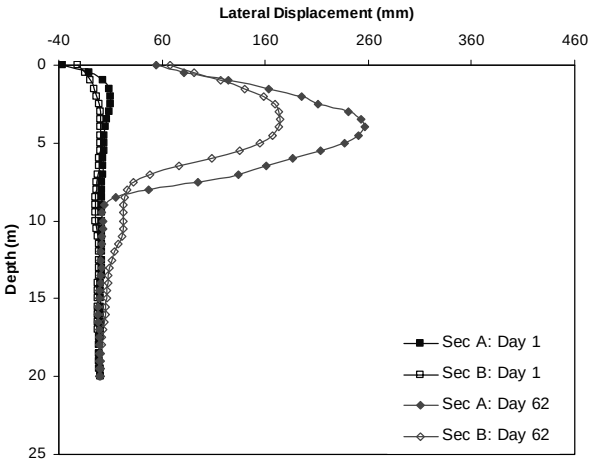

Fig. 12(a) Variation of lateral displacements in Section A and Section B (before end of construction) at location XX

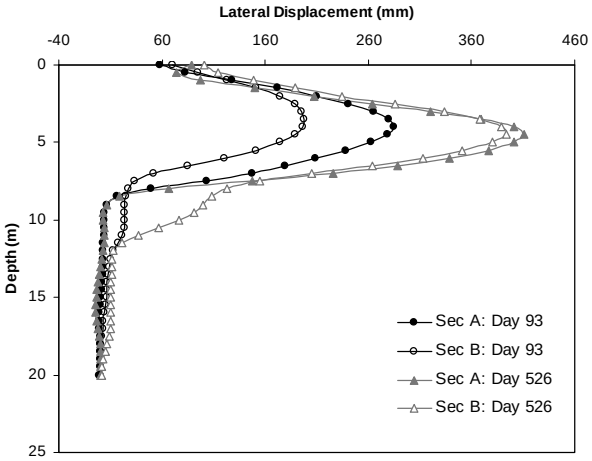

Fig. 12(b) Variation of lateral displacements in Section A and Section B (after end of construction) at location XX

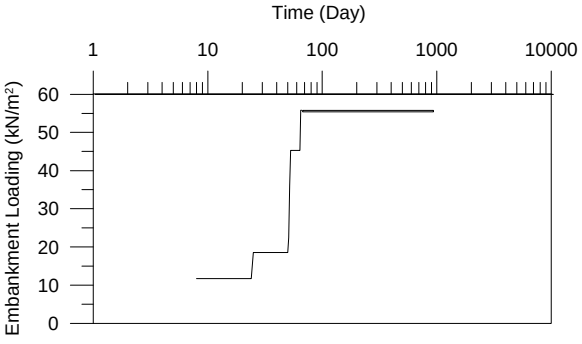

Fig. 13 Embankment loading (kN/m^2) with time (days) in Section A

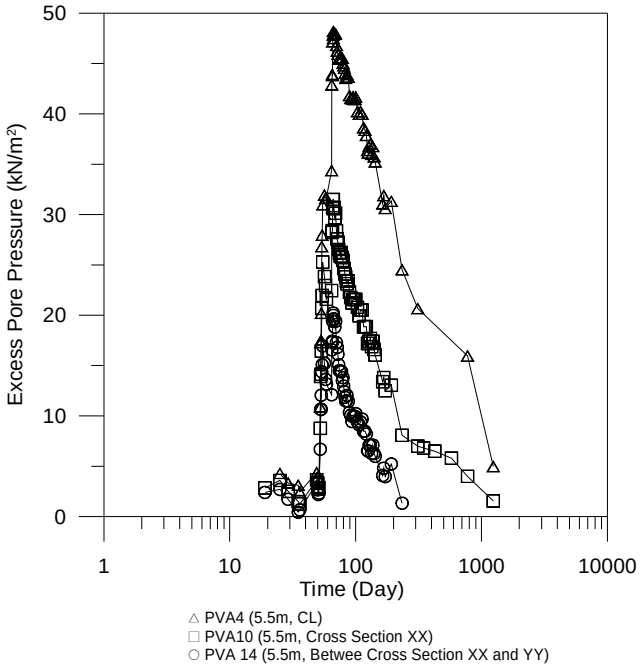

Fig. 14 Variation of excess pore pressure with time in Section A (Piezometers PVA4, PVA10 and PVA14)

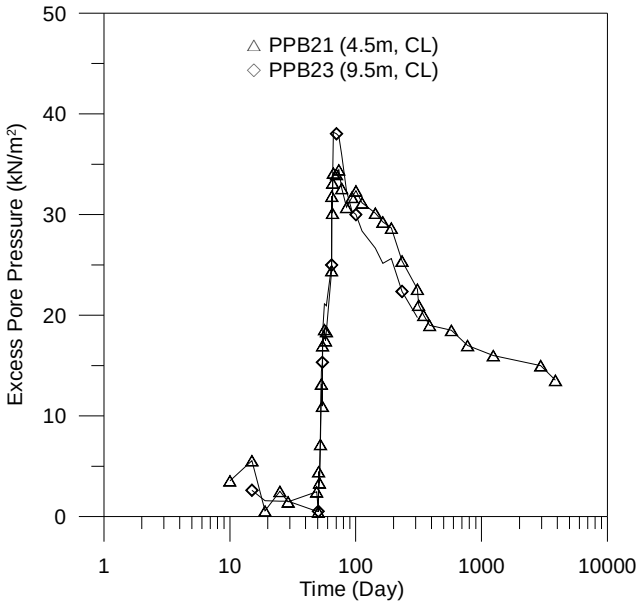

Fig. 15 Variation of excess pore pressure with time in Section B (Piezometers PPB21 and PPB23)

For Section C, the excess pore pressures and their dissipation with time are shown in Fig. 16 based on the excess pore pressures measured by piezometers PVC39 and PVC40 located at depths of 7m and 10m respectively are shown.

The pore pressure dissipation in Section A with closer PVD is faster than the corresponding dissipation in Section C with wider PVD spacing and this again is faster than Section B with no PVD. The minimum acceptable drain spacing as reported elsewhere is also in the range of 1.0 m; this is to prevent excessive smearing effects at very close spacing lesser than 1.0m.

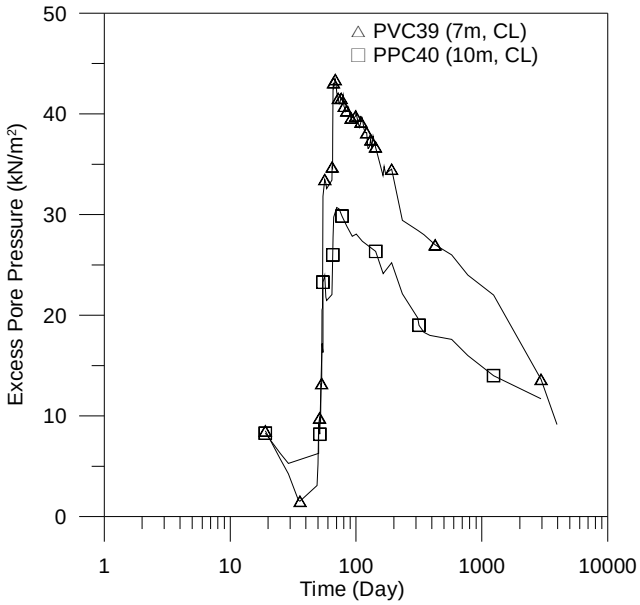

Fig. 16 Variation of excess pore pressure with time in Section C (Piezometers PPVC39 and PPC40)

4 CONCLUDING REMARKS

This paper presents the laboratory and field behaviour of soft clay deposit at a test site in Southeast Queensland, as well as the behaviour of embankment on soft ground constructed with and without ground improvement. From the different analyses performed in this study, the following conclusions can be made:

1. The laboratory results indicated that soft clays deposit in the studied areas is very soft and highly compressible. The under lying soils below the trial embankment can be considered as normally to slightly overconsolidated soil.
2. Maximum lateral displacement of the order of 400mm was observed and the lateral displacement is contained in the upper 8 – 10m of soft silty clay, which is susceptible to shear failure
3. The pore pressure dissipation indicated that the settlement measured is largely of the consolidation type.

Due to space limitations, finite element analysis and creep effects have not been discussed and will be reported elsewhere.

ACKNOWLEDGMENTS

The authors wish to express appreciation to Geotechnical Branch of Queensland Department of Main Roads, for their support in providing the soil samples, and the permission to use the data presented in this paper.

REFERENCES

Asaoka, A., (1978). Observation procedure of settlement prediction. *Soils and Foundations*, Vol. 18, No. 4, pp. 87-101.